Global View of Cosmic Ray Data

In the Era of High Resolution Measurements

Serap Tilav

Bartol Research Institute

University of Delaware

UHECR2014 Oct /12-15/2014 Springdale Utah

When looked in detail the CR spectrum is not a simple power law

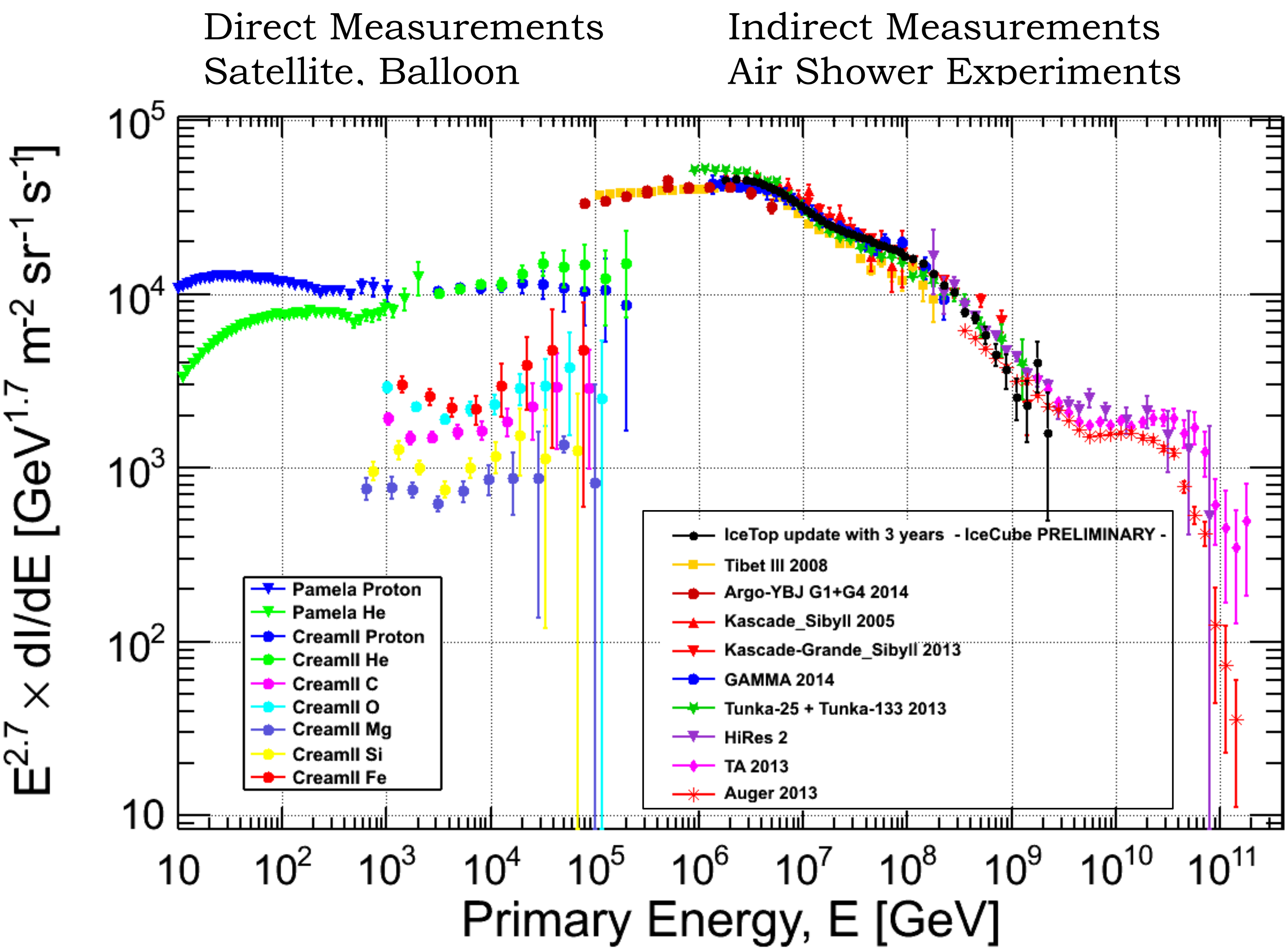

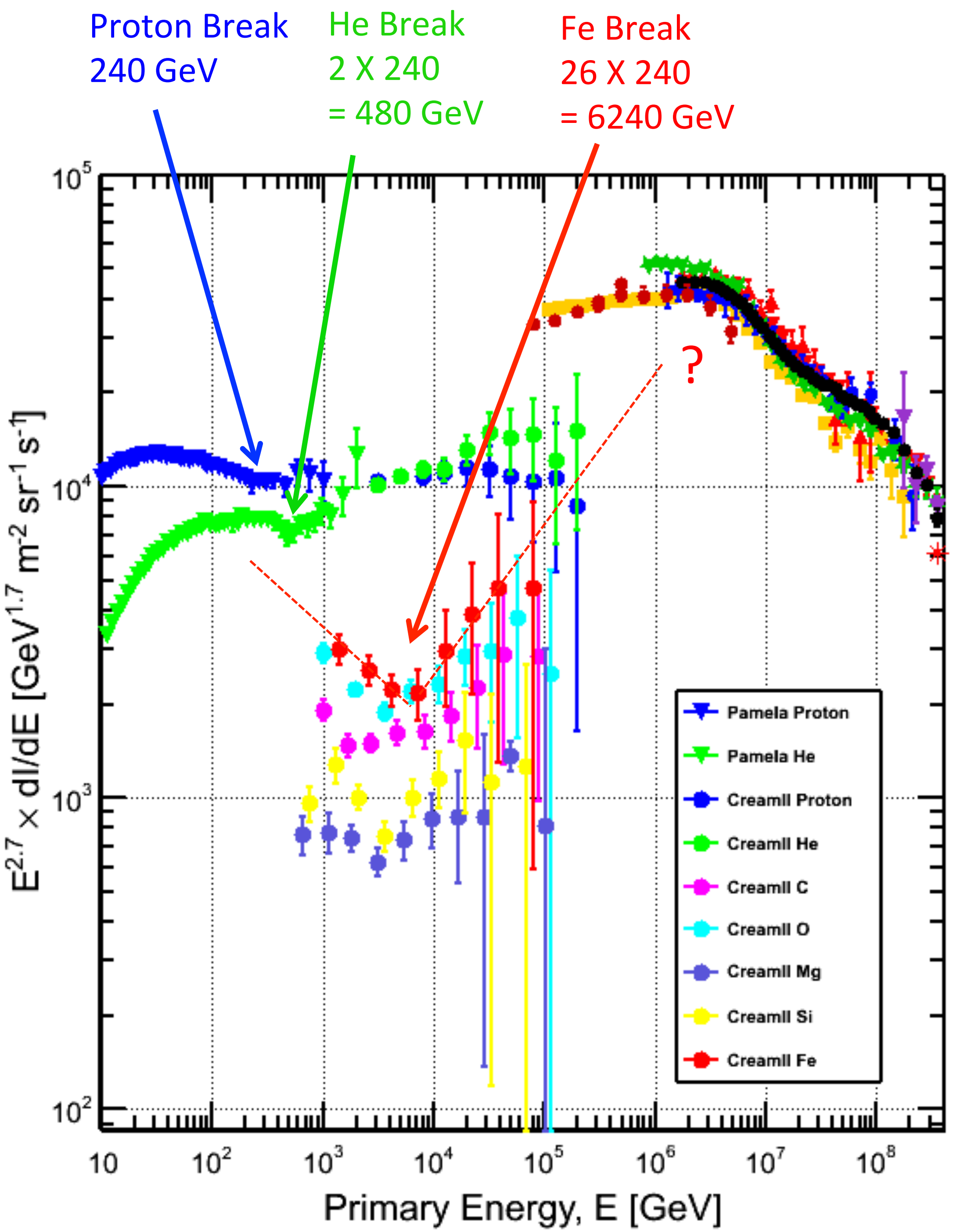

PAMELA /ATIC/ CREAM
reveal rigidity dependent
spectral breaks
and
remarkable hardening
after the breaks

Perfect demonstration
of Peters cycle:

When protons accelerated to E^p_{max} a nucleus with Ze will be accelerated up to
$E^z_{max} = Ze \times R = Z \times E^p_{max}$

where magnetic rigidity
$R = Pc/Ze$

Bernard Peters 1961

Spectral Indices of the hard component

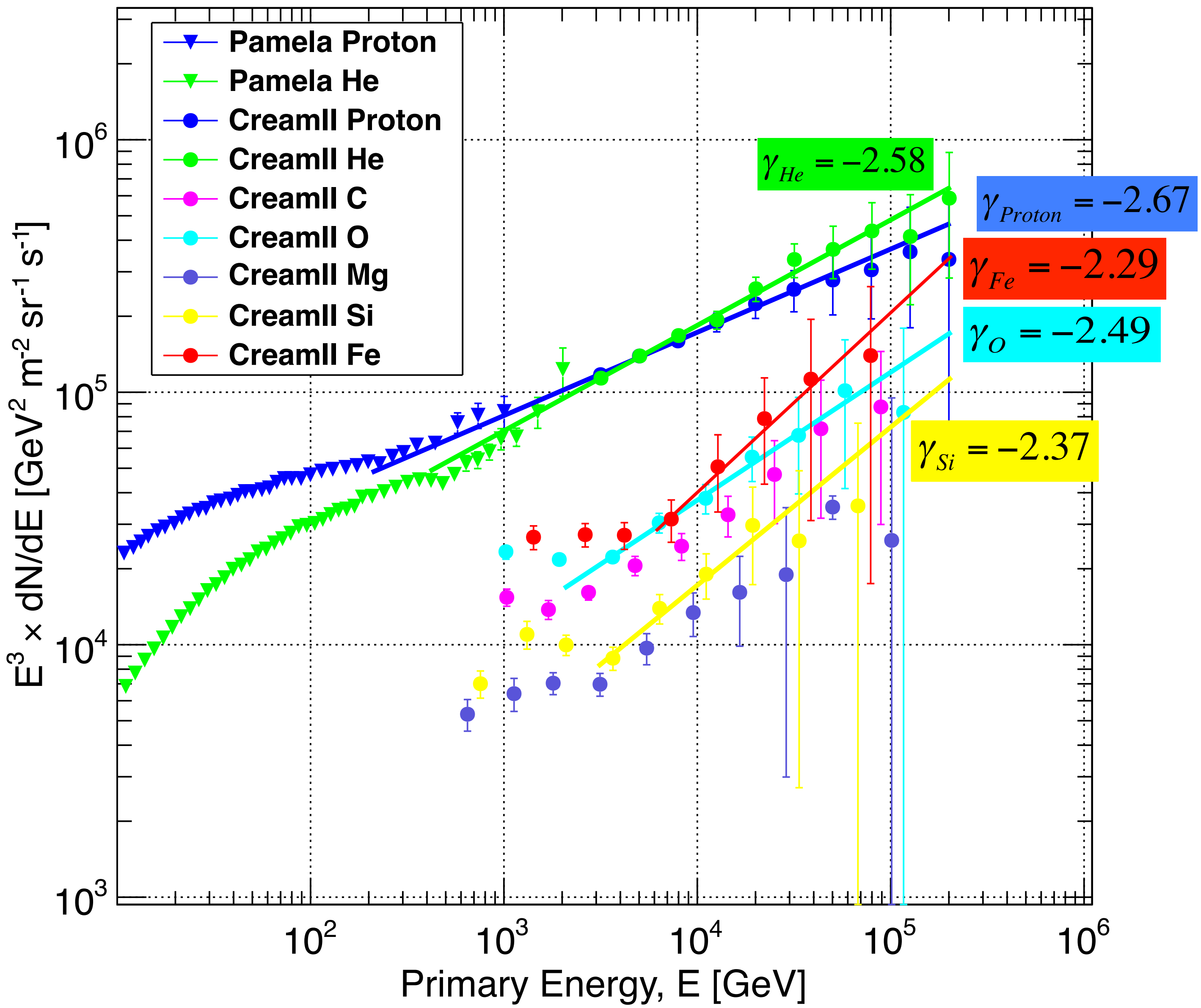

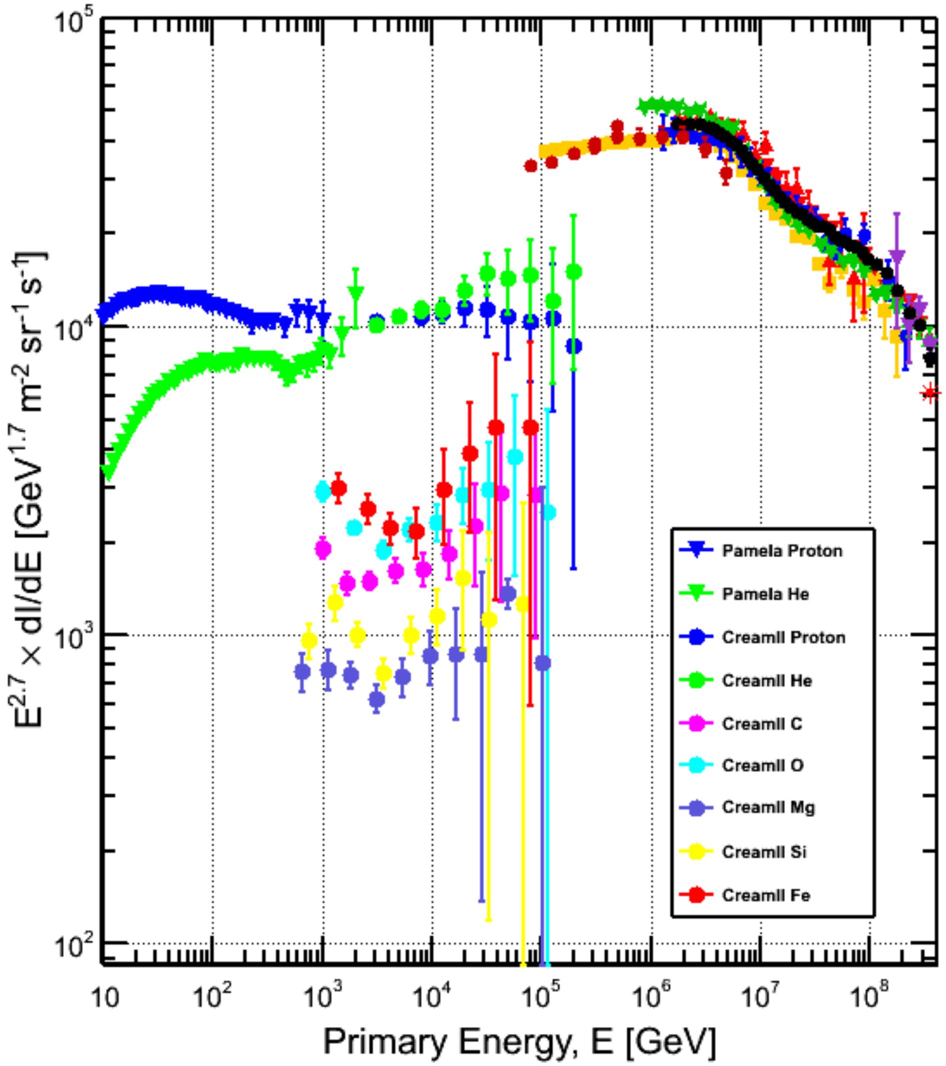

Fit the elemental spectrum with Gaisser's formulation of Peters cycle

$$E\frac{dN}{dE} = \sum_{i}^{elements} A_i E^{-\gamma_i} e^{-\frac{E}{Z_i E_{cutoff}}}$$

A	Amplitude
γ	spectral index
E_{cutoff}	cut-off energy

Above the knee use <lnA> as guidance

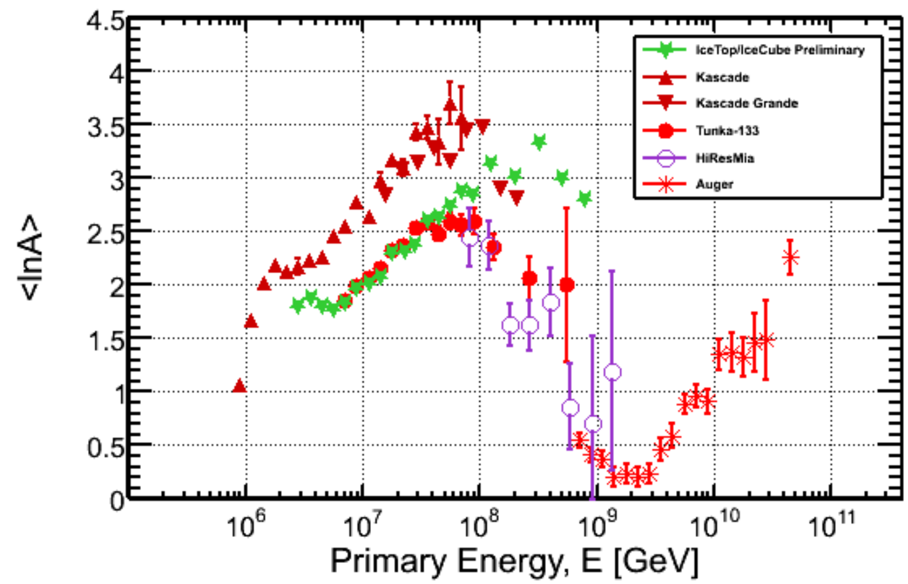

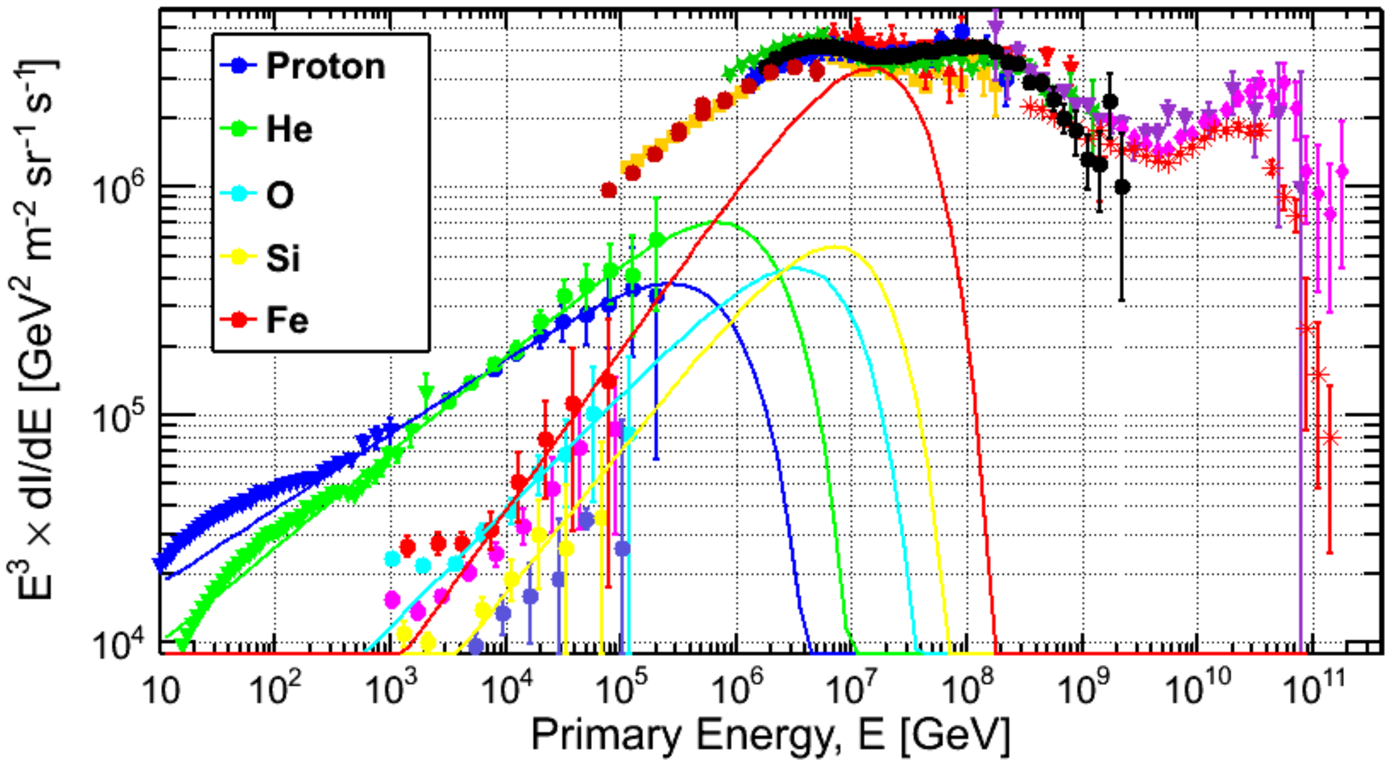

Amplitudes and indexes of all elements are defined by the CreamII data. Only the cutoffs need to be fit.

Fe spectrum is the key to the whole puzzle.

The Cream Fe data, when extended with the same index up to an energy where it makes 100% of the all particle spectrum, defines the maximum cut off energy for Fe.

This point turns out to be 20.8 PeV.

If Fe cuts off at 20.8 PeV ➔ Proton will cut off at 20800/26 =800 TeV

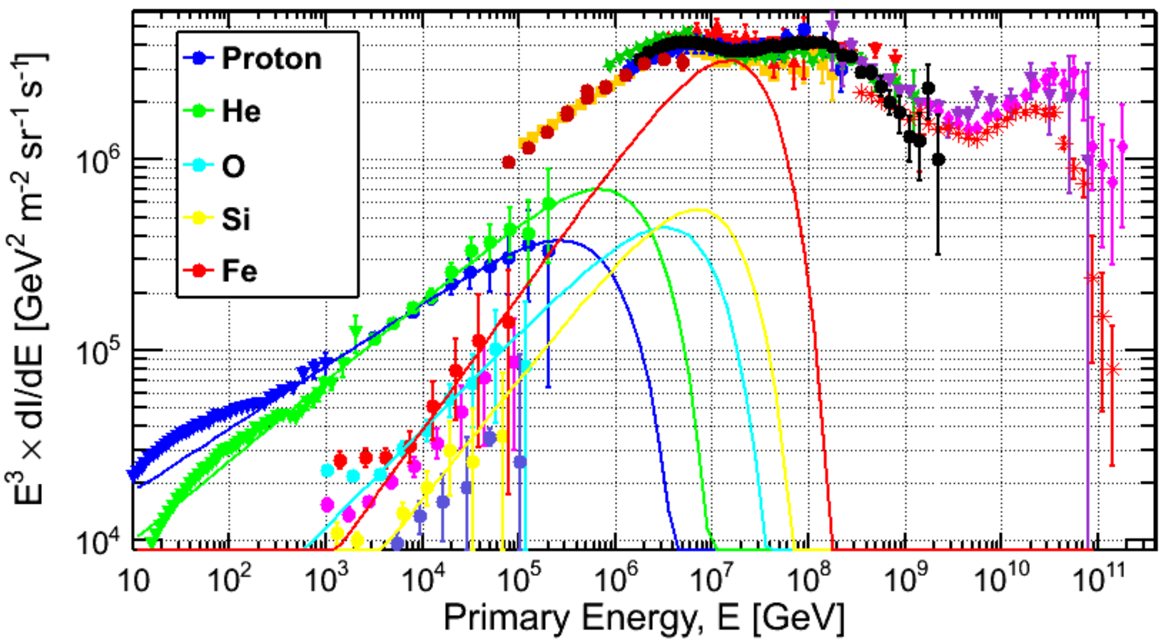

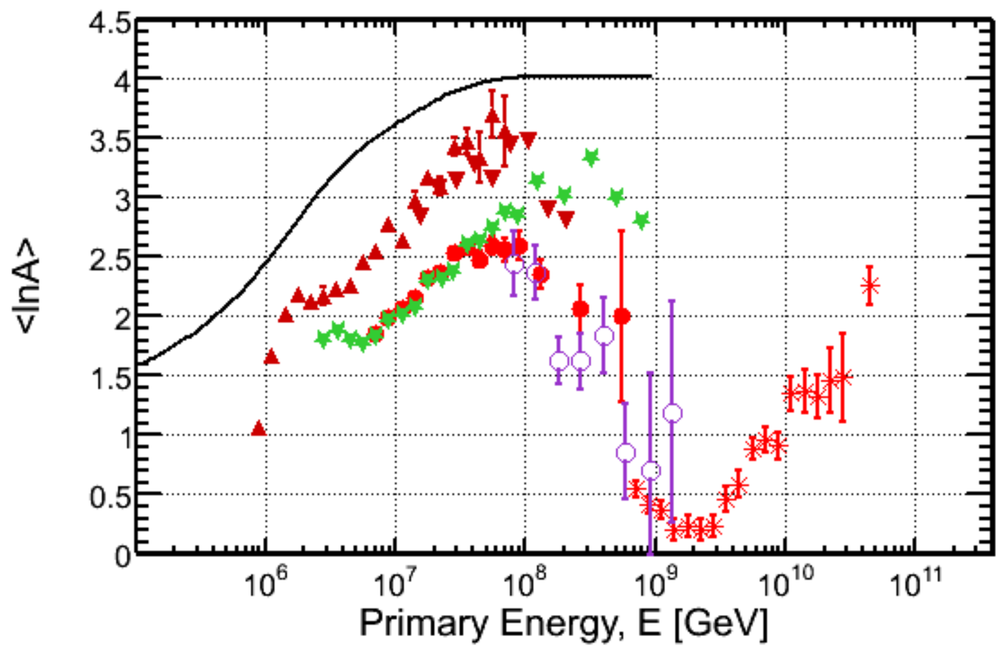

However

<lnA> data tells us
the knee is not 100% Fe.

Since the amplitudes are locked
by the Cream data,
the only way to fit <lnA> is
to bring the cutoff energy down

and fill the rest with elements
of a new Peters cycle
(a new population of particles)

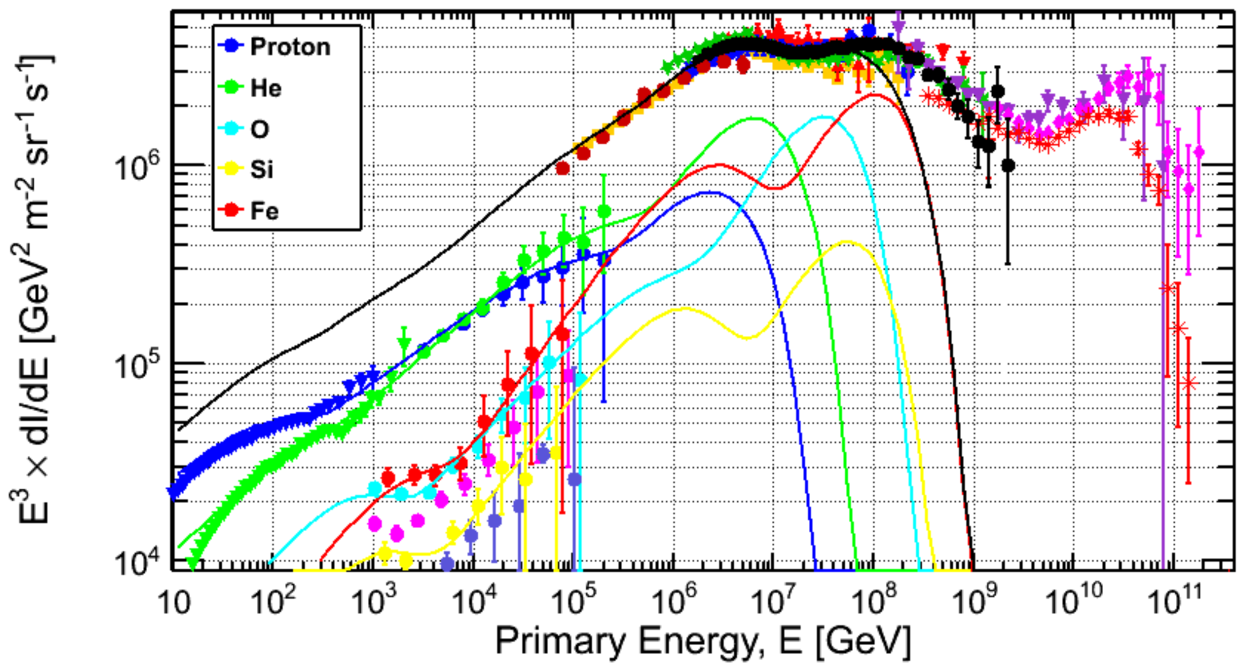

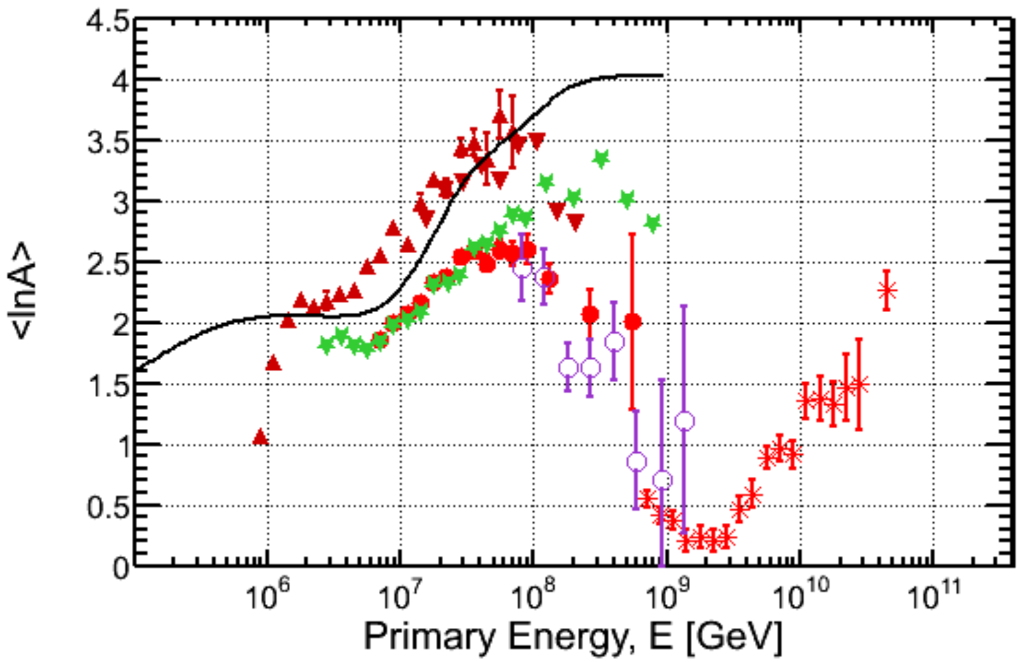

insert another Peter's cycle overlapping with the previous one until the best agreement with lnA is reached and constrained by the spectrum

$90 \text{ TeV} < E^1_{cutoff} < 150 \text{ TeV}$

and

$2 \text{ PeV} < E^2_{cutoff} < 4.5 \text{ PeV}$ with much harder spectral indices

$\gamma_{Proton} = -2.3$ $\gamma_{He} = -2.2$

$\gamma_{CNO} = -2.0$ $\gamma_{Si} = -2.0$ $\gamma_{Fe} = -2.0$

The comic ray knee is the intersection of two different source populations

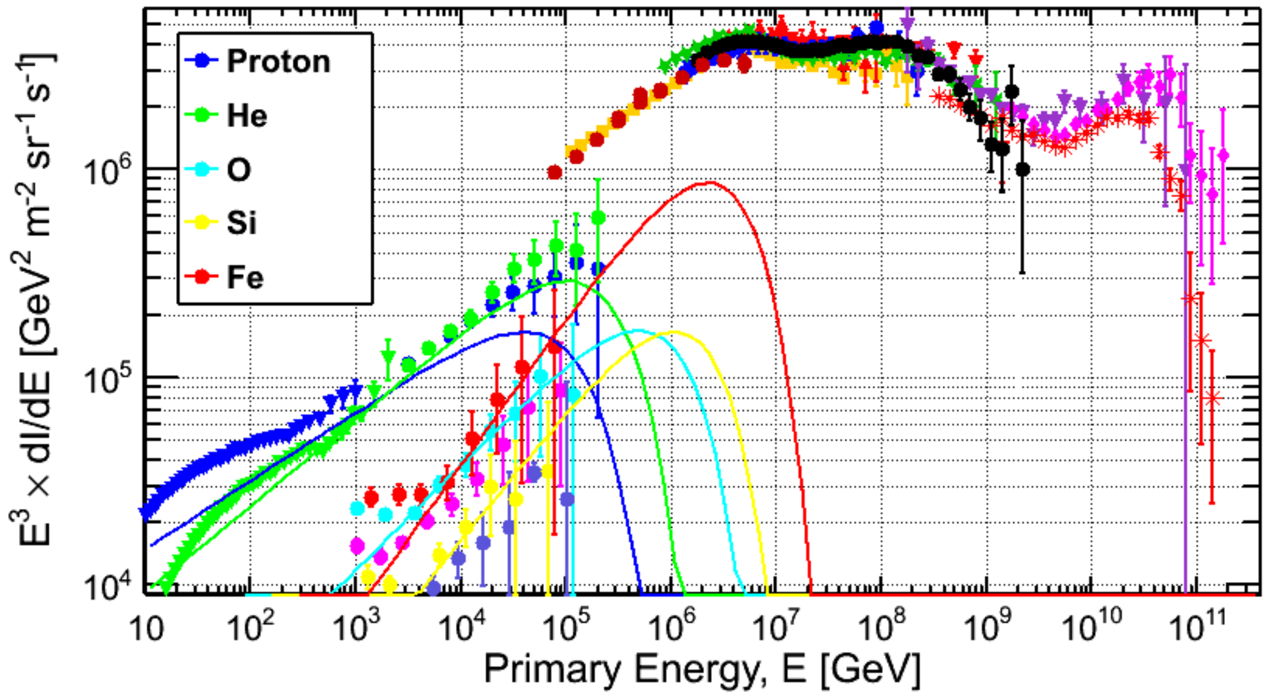

Cycle 1 alone

E^{p}_{cutoff} = 120 TeV

E^{Fe}_{cutoff} = *26 x* 120 TeV = 3.1 PeV

The CR Knee

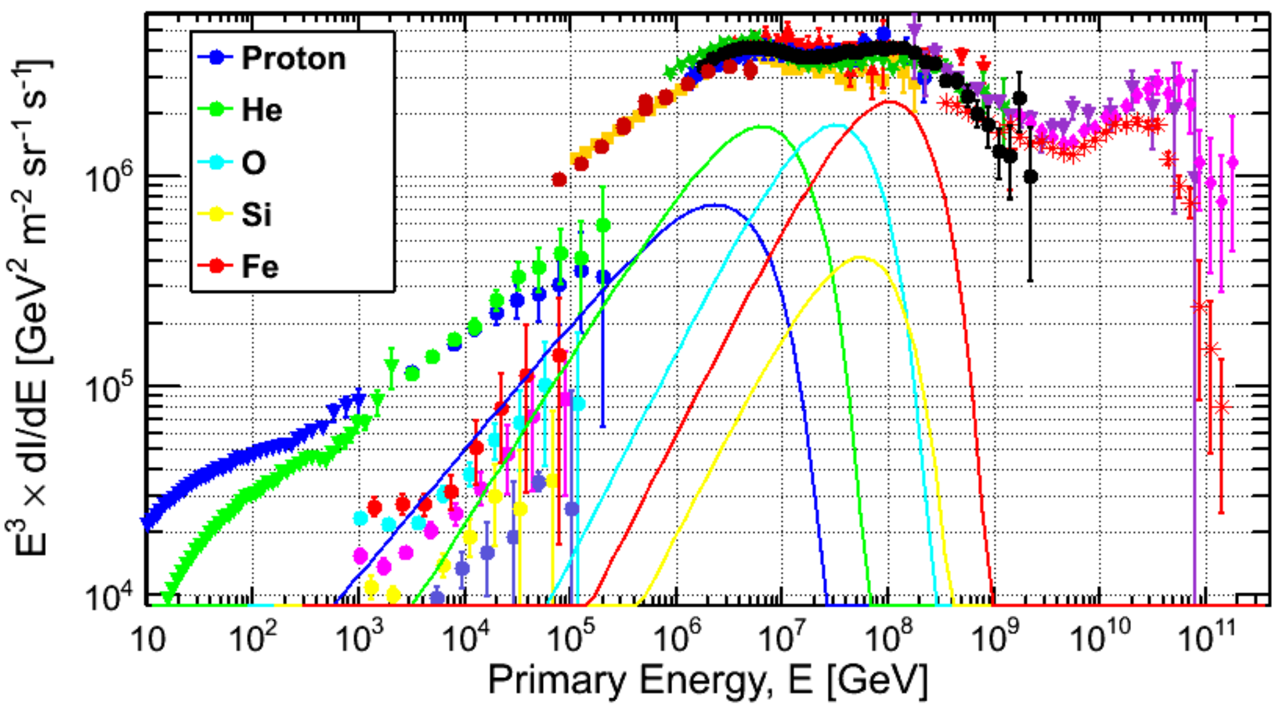

Cycle 2 alone

E^{p}_{cutoff} = 4 PeV

E^{Fe}_{cutoff} = *26 x* 4 PeV = 104 PeV

Proceed with the same method to inject another Peters cycle for UHE

- Try to fit Auger's composition as Cycle 3
- However, a gap is left between Cycle 2 and 3 and lnA turns to light too soon. There has to be some heavy elements at least upto 300 PeV.
  ➔ include ultraheavy element groups as extension of Cycle 2
  (as inspired by the lowE GCR measurements)

without ultraheavy nuclei

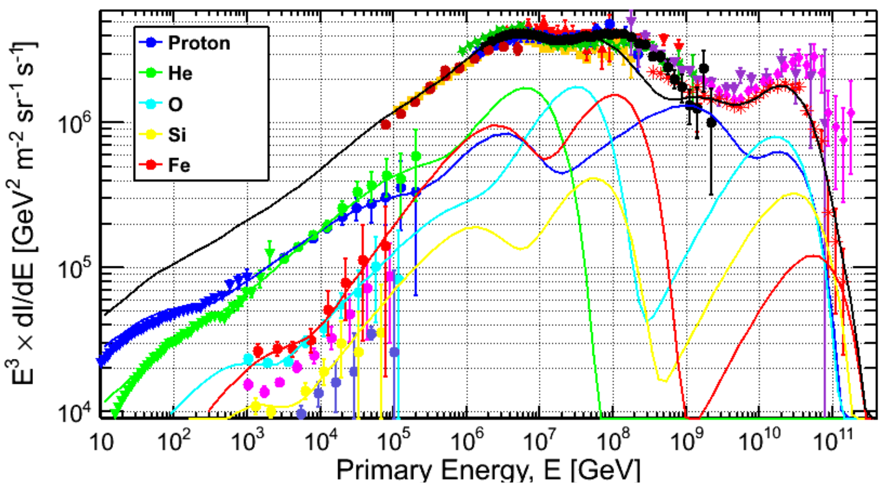

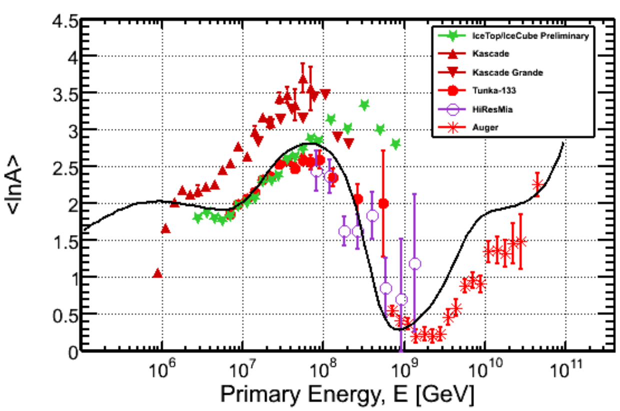

with ultraheavy nuclei

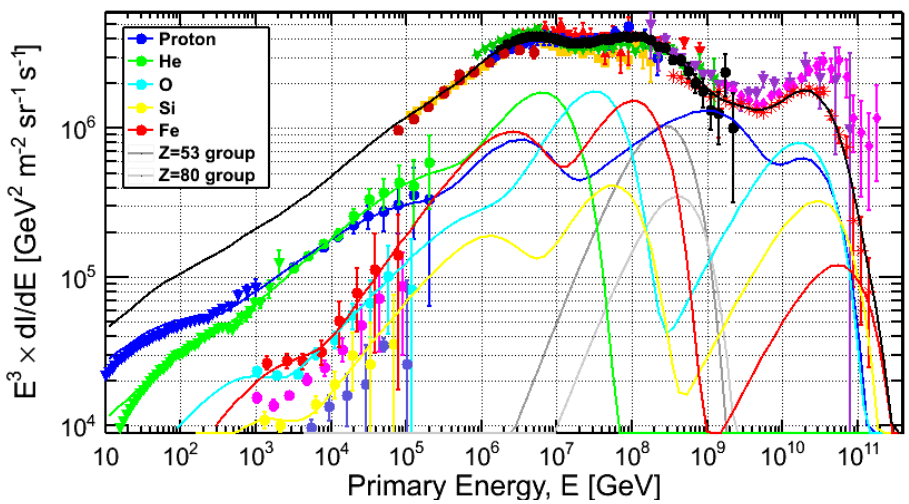

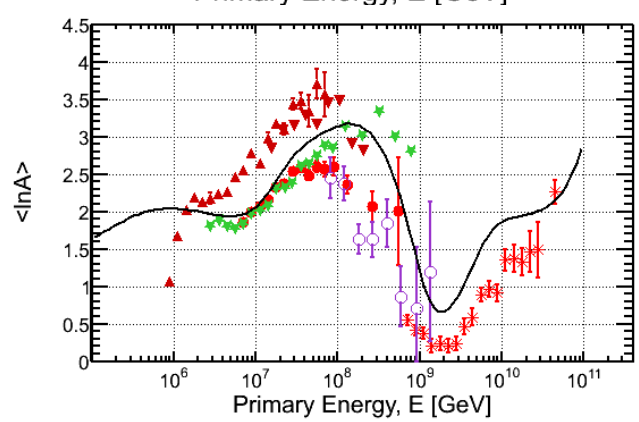

Auger fits to standard Peters cycle

with Proton cut off at 2.1 EeV (index=2.6)

No Helium could be accommodated

Oxygen is dominant,

but there has to be some Si and Fe as well

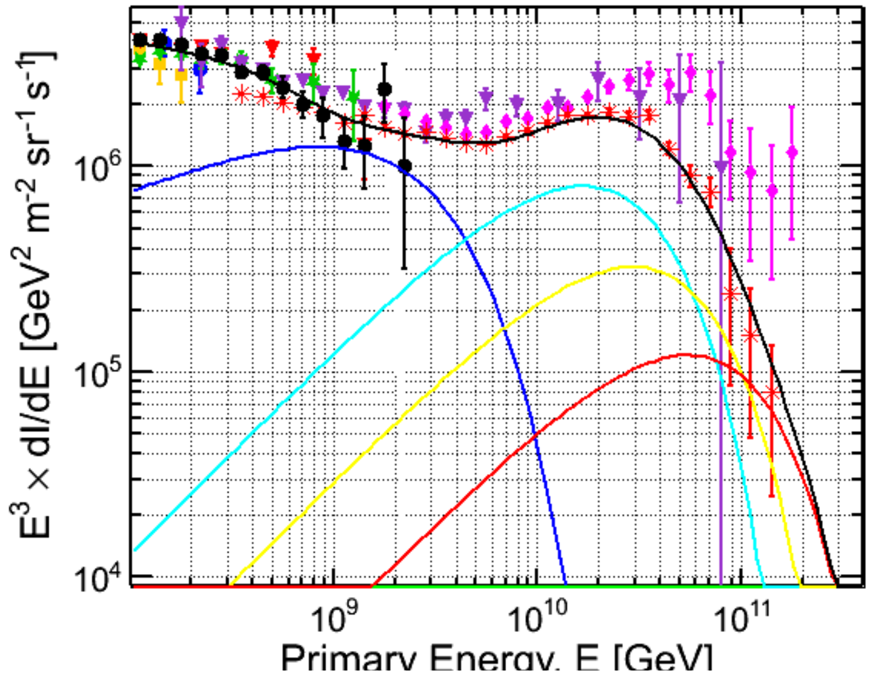

BUT: There is an EXTRA Proton

which is not part of the standard cycle

➔ this Proton cuts off ~ 20 EeV (index=2.0)

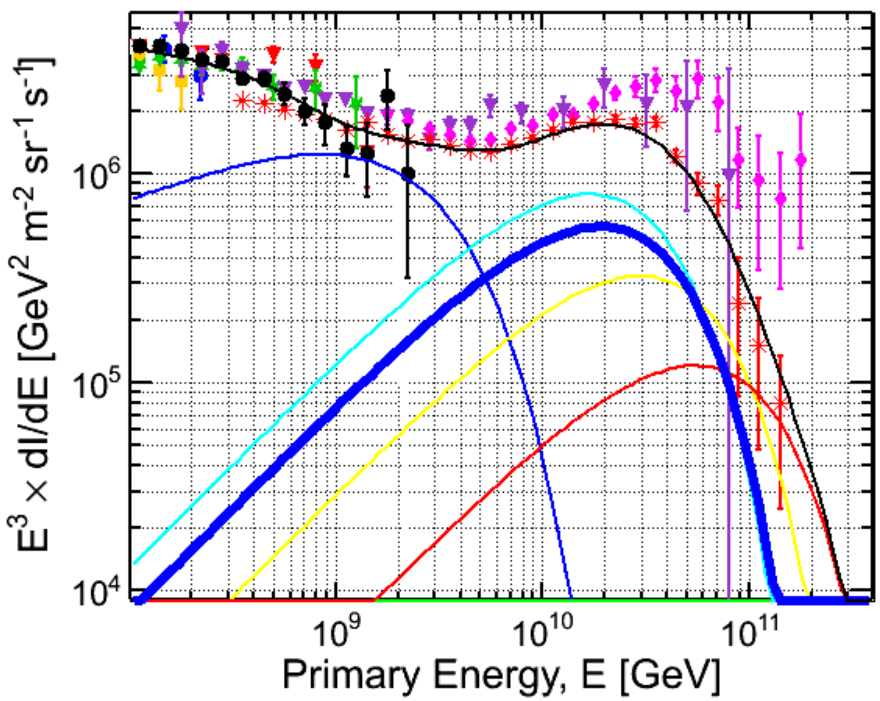

Compare with the Auger results: best performance is with EPOS-LHC

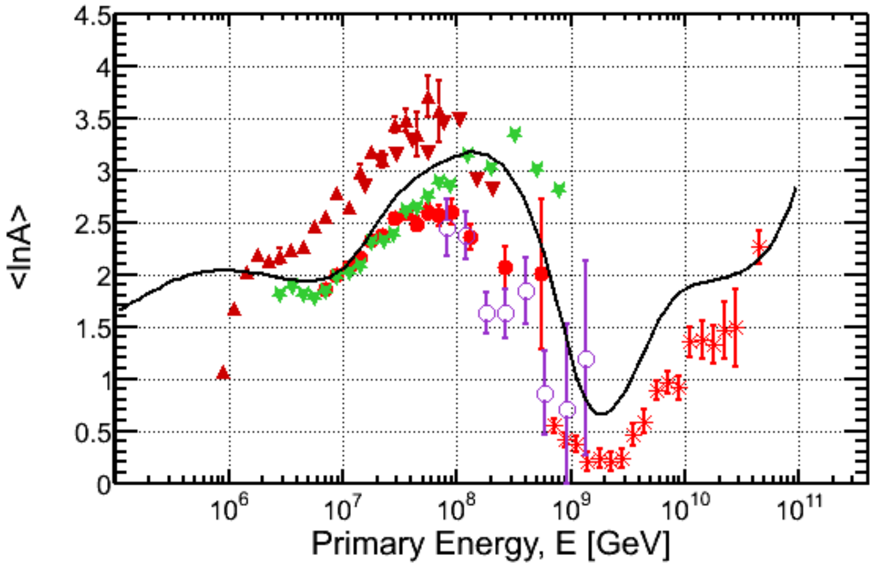

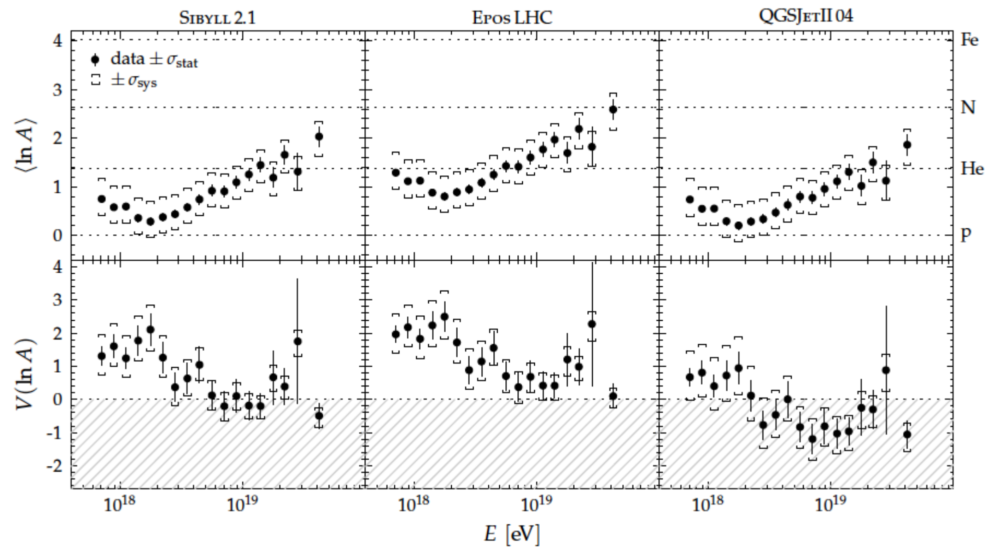

Figure 14: Average of the logarithmic mass and its variance estimated from data using different interaction models. The non-physical region of negative variance is indicated as the gray dashed region.

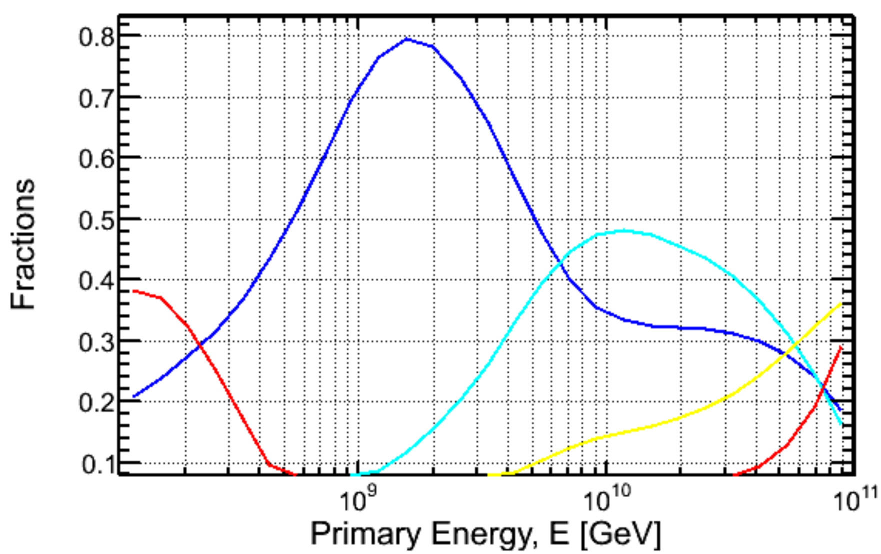

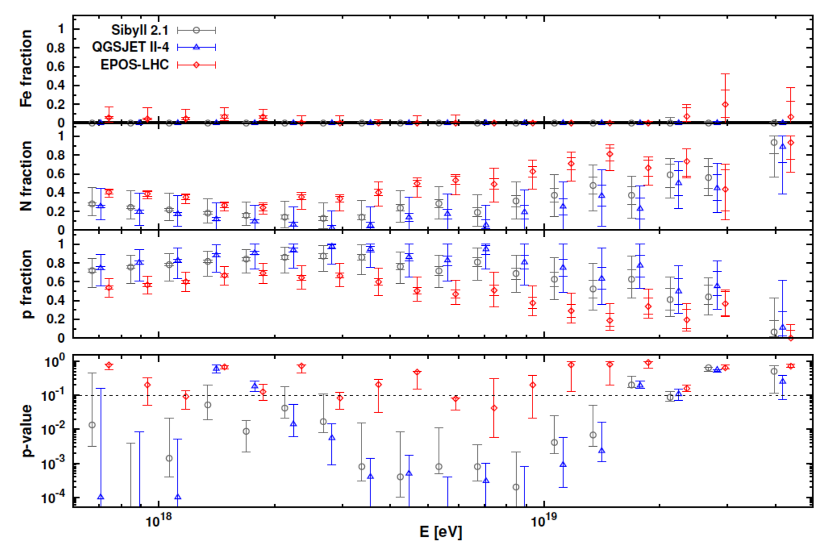

FIG. 3: Fitted fraction and quality for the scenario of a complex mixture of protons, nitrogen nuclei, and iron nuclei. The upper panels show the species fractions and the lower panel shows the p-values.

Compare Auger and TA

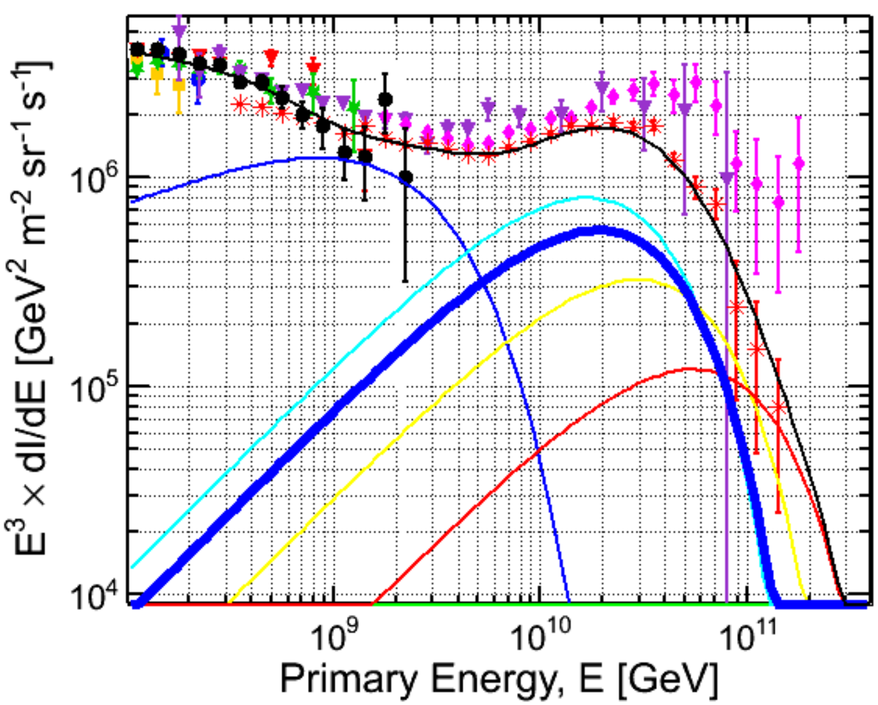

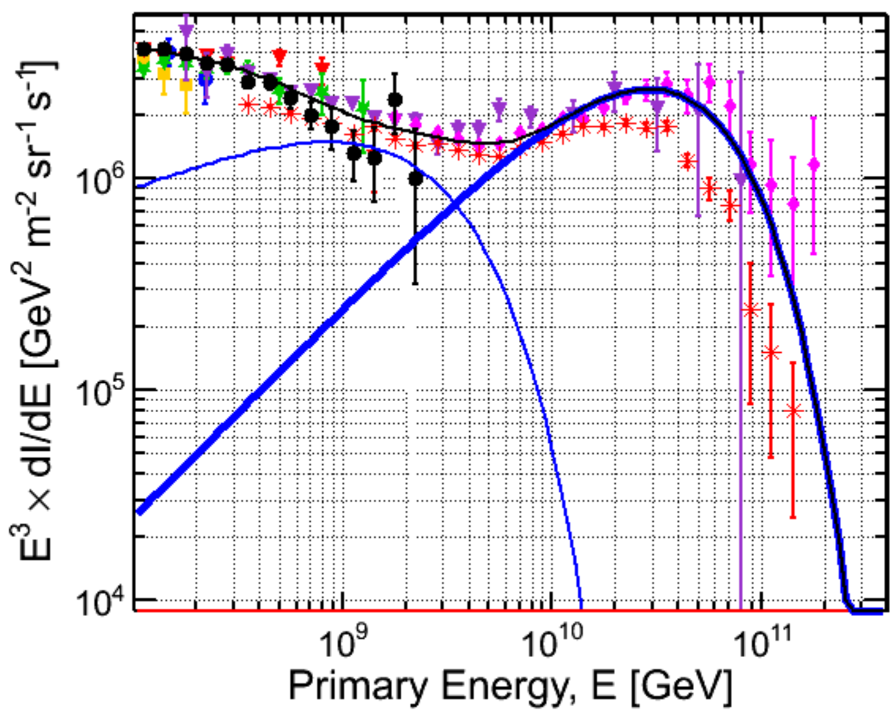

Auger sees heavy elements under extra-galactic Proton

TA sees all extra-galactic Proton (are the elements there in undetectable levels?)

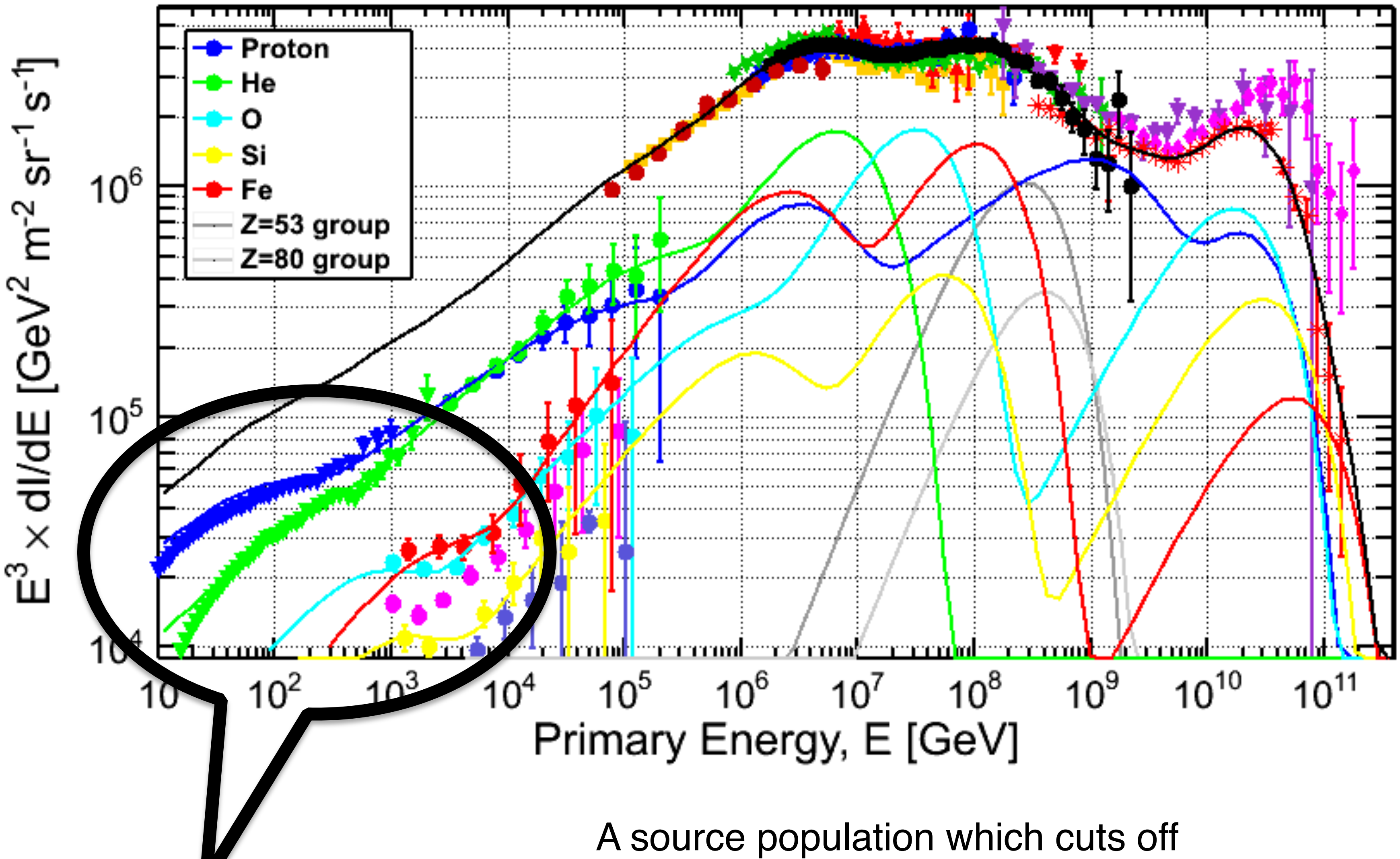

There is yet another Peter's cycle here

A source population which cuts off around 100 GeV will explain the PAMELA break, which is the overlap between this population and the harder classic supernovae component setting in.

FERMI-LAT

SCIENCE VOL 339 15 FEBRUARY 2013

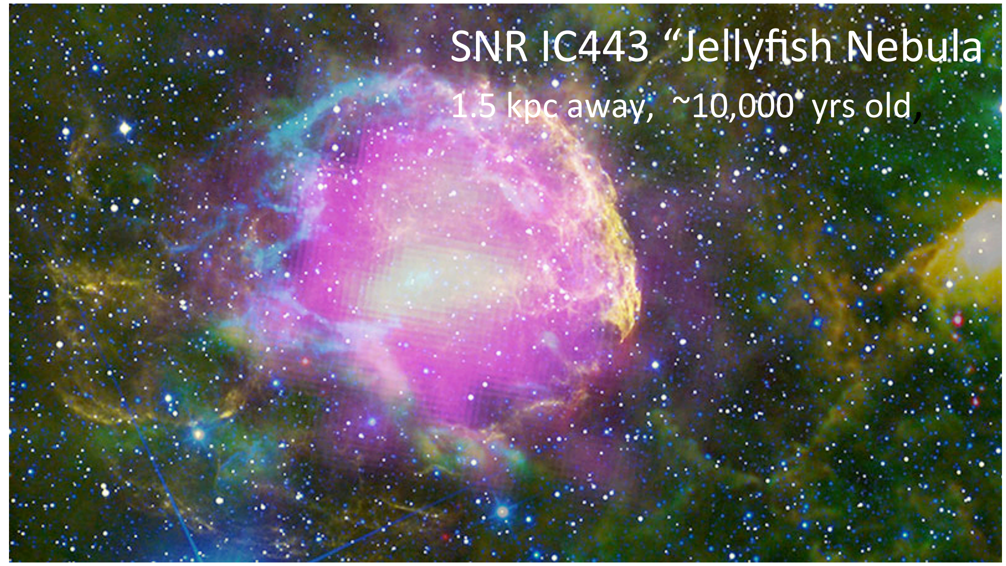

Detection of the Characteristic Pion-Decay Signature in Supernova Remnants

M. Ackermann,[1] M. Ajello,[2] A. Allafort,[3] L. Baldini,[4] J. Ballet,[5] G. Barbiellini,[6,7] M. G. Baring,[8] D. Bastieri,[9,10] K. Bechtol,[3] R. Bellazzini,[11] R. D. Blandford,[3] E. D. Bloom,[3] E. Bonamente,[12,13] A. W. Borgland,[3] E. Bottacini,[3] T. J. Brandt,[14] J. Bregeon,[11] M. Brigida,[15,16] P. Bruel,[17] R. Buehler,[3] G. Busetto,[9,10] S. Buson,[9,10] G. A. Caliandro,[18] R. A. Cameron,[3] P. A. Caraveo,[19] J. M. Casandjian,[5] C. Cecchi,[12,13] Ö. Çelik,[14,20,21] E. Charles,[3] S. Chaty,[5] R. C. G. Chaves,[5] A. Chekhtman,[22] C. C. Cheung,[23] J. Chiang,[3] G. Chiaro,[24] A. N. Cillis,[14,25] S. Ciprini,[13,26] R. Claus,[3] J. Cohen-Tanugi,[27] L. R. Cominsky,[28] J. Conrad,[29,30,31] S. Corbel,[5,32] S. Cutini,[33] F. D'Ammando,[12,34,35] A. de Angelis,[36] F. de Palma,[15,16] C. D. Dermer,[37] E. do Couto e Silva,[3] P. S. Drell,[3] A. Drlica-Wagner,[3] L. Falletti,[27] C. Favuzzi,[15,16] E. C. Ferrara,[14] A. Franckowiak,[3] Y. Fukazawa,[38] S. Funk,[3*] P. Fusco,[15,16] F. Gargano,[16] S. Germani,[12,13] N. Giglietto,[15,16] P. Giommi,[33] F. Giordano,[15,16] M. Giroletti,[39] T. Glanzman,[3] G. Godfrey,[3] I. A. Grenier,[5] M.-H. Grondin,[40,41] J. E. Grove,[37] S. Guiriec,[14] D. Hadasch,[18] Y. Hanabata,[38] A. K. Harding,[14] M. Hayashida,[3,42] K. Hayashi,[38] E. Hays,[14] J. W. Hewitt,[14] A. B. Hill,[3,43] R. E. Hughes,[44] M. S. Jackson,[30,45] T. Jogler,[3] G. Jóhannesson,[46] A. S. Johnson,[3] T. Kamae,[3] J. Kataoka,[47] J. Katsuta,[3] J. Knödlseder,[48,49] M. Kuss,[11] J. Lande,[3] S. Larsson,[29,30,50] L. Latronico,[51] M. Lemoine-Goumard,[52,53] F. Longo,[6,7] F. Loparco,[15,16] M. N. Lovellette,[37] P. Lubrano,[12,13] G. M. Madejski,[3] F. Massaro,[3] M. Mayer,[1] M. N. Mazziotta,[16] J. E. McEnery,[14,54] J. Mehault,[27] P. F. Michelson,[3] R. P. Mignani,[55] W. Mitthumsiri,[3] T. Mizuno,[56] A. A. Moiseev,[20,54] M. E. Monzani,[3] A. Morselli,[57] I. V. Moskalenko,[3] S. Murgia,[3] T. Nakamori,[47] R. Nemmen,[14] E. Nuss,[27] M. Ohno,[58] T. Ohsugi,[56] N. Omodei,[3] M. Orienti,[39] E. Orlando,[3] J. F. Ormes,[59] D. Paneque,[3,60] J. S. Perkins,[14,21,20,61] M. Pesce-Rollins,[11] F. Piron,[27] G. Pivato,[10] S. Rainò,[15,16] R. Rando,[9,10] M. Razzano,[11,62] S. Razzaque,[22] A. Reimer,[3,63] O. Reimer,[3,63] S. Ritz,[62] C. Romoli,[10] M. Sánchez-Conde,[3] A. Schulz,[1] C. Sgrò,[11] P. E. Simeon,[3] E. J. Siskind,[64] D. A. Smith,[52] G. Spandre,[11] P. Spinelli,[15,16] F. W. Stecker,[14,65] A. W. Strong,[66] D. J. Suson,[67] H. Tajima,[3,68] H. Takahashi,[38] T. Takahashi,[58] T. Tanaka,[3,69*] J. G. Thayer,[3] J. B. Thayer,[3] D. J. Thompson,[14] S. E. Thorsett,[70] L. Tibaldo,[9,10] O. Tibolla,[71] M. Tinivella,[11] E. Troja,[14,72] Y. Uchiyama,[3*] T. L. Usher,[3] J. Vandenbroucke,[3] V. Vasileiou,[27] G. Vianello,[3,73] V. Vitale,[57,74] A. P. Waite,[3] M. Werner,[63] B. L. Winer,[44] K. S. Wood,[37] M. Wood,[3] R. Yamazaki,[75] Z. Yang,[29,30] S. Zimmer[29,30]

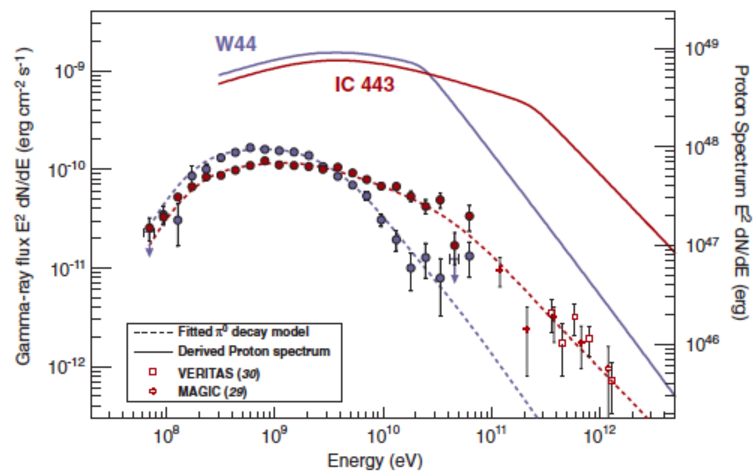

Fig. 3. Proton and gamma-ray spectra determined for IC 443 and W44. Also shown are the broadband spectral flux points derived in this study, along with TeV spectral data points for IC 443 from MAGIC (*29*) and VERITAS (*30*). The curvature evident in the proton distribution at ~2 GeV is a consequence of the display in energy space (rather than momentum space). Gamma-ray spectra from the protons were computed using the energy-dependent cross section parameterized by (*32*). We took into account accelerated nuclei (heavier than protons) as well as nuclei in the target gas by applying an enhancement factor of 1.85 (*33*). Note that models of the gamma-ray production via *pp* interactions have some uncertainty. Relative to the model adopted here, an alternative model of (*6*) predicts ~30% less photon flux near 70 MeV; the two models agree with each other to better than 15% above 200 MeV. The proton spectra assume average gas densities of $n = 20\ \mathrm{cm}^{-3}$ (IC 443) and $n = 100\ \mathrm{cm}^{-3}$ (W44) and distances of 1.5 kpc (IC 443) and 2.9 kpc (W44).

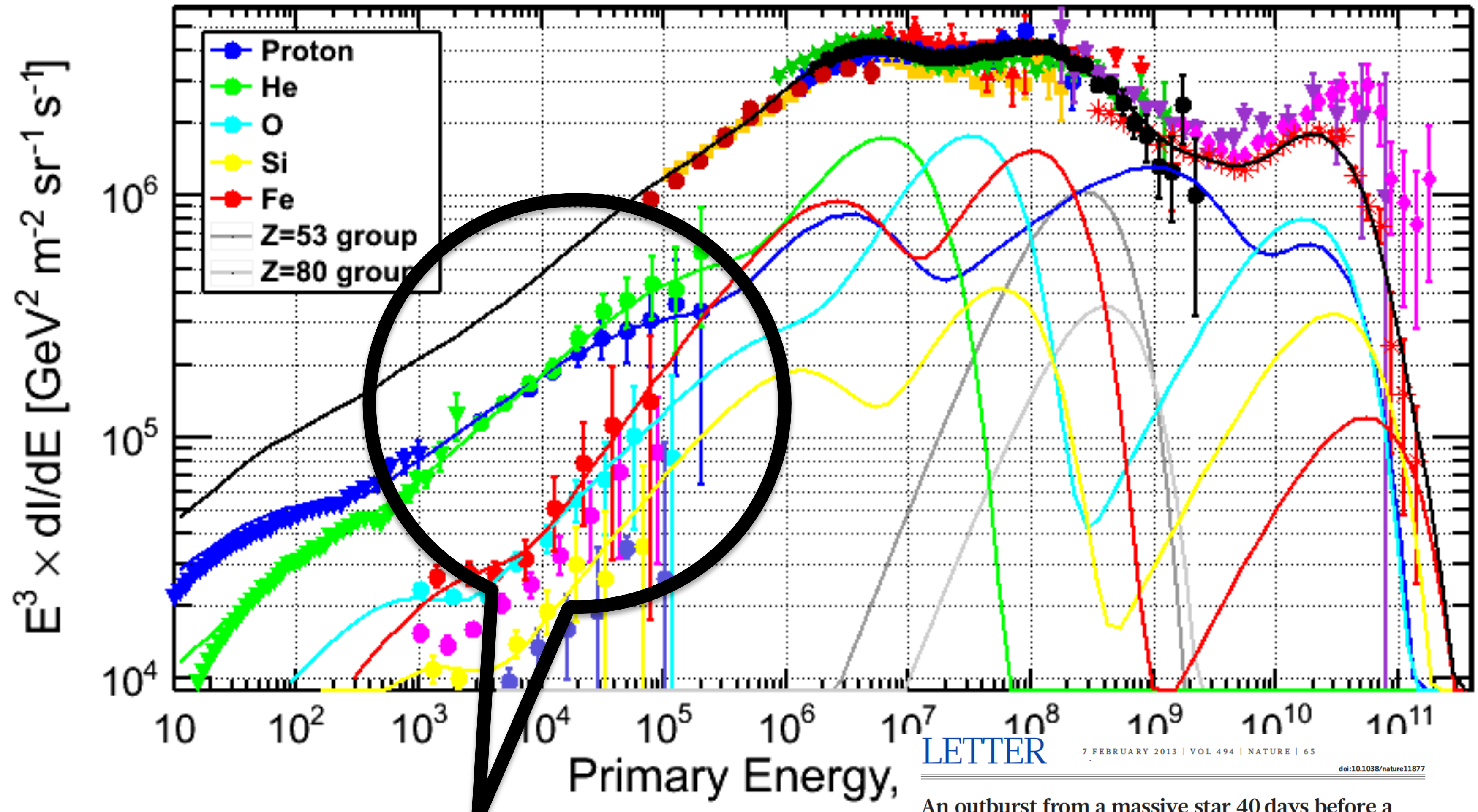

The classical supernovae
cutting around 100 TeV

Massive stars, circumstellar ejecta

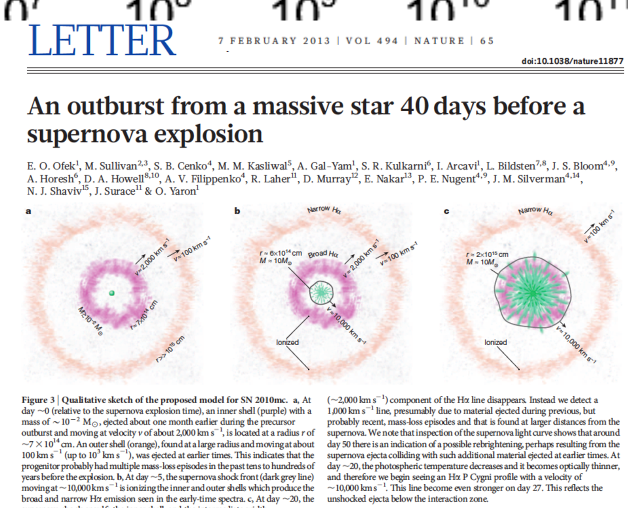

LETTER

7 FEBRUARY 2013 | VOL 494 | NATURE | 65

doi:10.1038/nature11877

An outburst from a massive star 40 days before a supernova explosion

E. O. Ofek[1], M. Sullivan[2,3], S. B. Cenko[4], M. M. Kasliwal[5], A. Gal-Yam[1], S. R. Kulkarni[6], I. Arcavi[1], L. Bildsten[7,8], J. S. Bloom[4,9], A. Horesh[6], D. A. Howell[8,10], A. V. Filippenko[4], R. Laher[11], D. Murray[12], E. Nakar[13], P. E. Nugent[4,9], J. M. Silverman[4,14], N. J. Shaviv[15], J. Surace[11] & O. Yaron[1]

Figure 3 | Qualitative sketch of the proposed model for SN 2010mc. **a**, At day ~0 (relative to the supernova explosion time), an inner shell (purple) with a mass of $\sim 10^{-2}\ M_\odot$, ejected about one month earlier during the precursor outburst and moving at velocity v of about 2,000 km s^{-1}, is located at a radius r of $\sim 7 \times 10^{14}$ cm. An outer shell (orange), found at a large radius and moving at about 100 km s^{-1} (up to 10^3 km s^{-1}), was ejected at earlier times. This indicates that the progenitor probably had multiple mass-loss episodes in the past tens to hundreds of years before the explosion. **b**, At day ~5, the supernova shock front (dark grey line) moving at ~10,000 km s^{-1} is ionizing the inner and outer shells which produce the broad and narrow Hα emission seen in the early-time spectra. **c**, At day ~20, the supernova shock engulfs the inner shell, and the intermediate-width (~2,000 km s^{-1}) component of the Hα line disappears. Instead we detect a 1,000 km s^{-1} line, presumably due to material ejected during previous, but probably recent, mass-loss episodes and that is found at larger distances from the supernova. We note that inspection of the supernova light curve shows that around day 50 there is an indication of a possible rebrightening, perhaps resulting from the supernova ejecta colliding with such additional material ejected at earlier times. At day ~20, the photospheric temperature decreases and it becomes optically thinner, and therefore we begin seeing an Hα P Cygni profile with a velocity of ~10,000 km s^{-1}. This line become even stronger on day 27. This reflects the unshocked ejecta below the interaction zone.

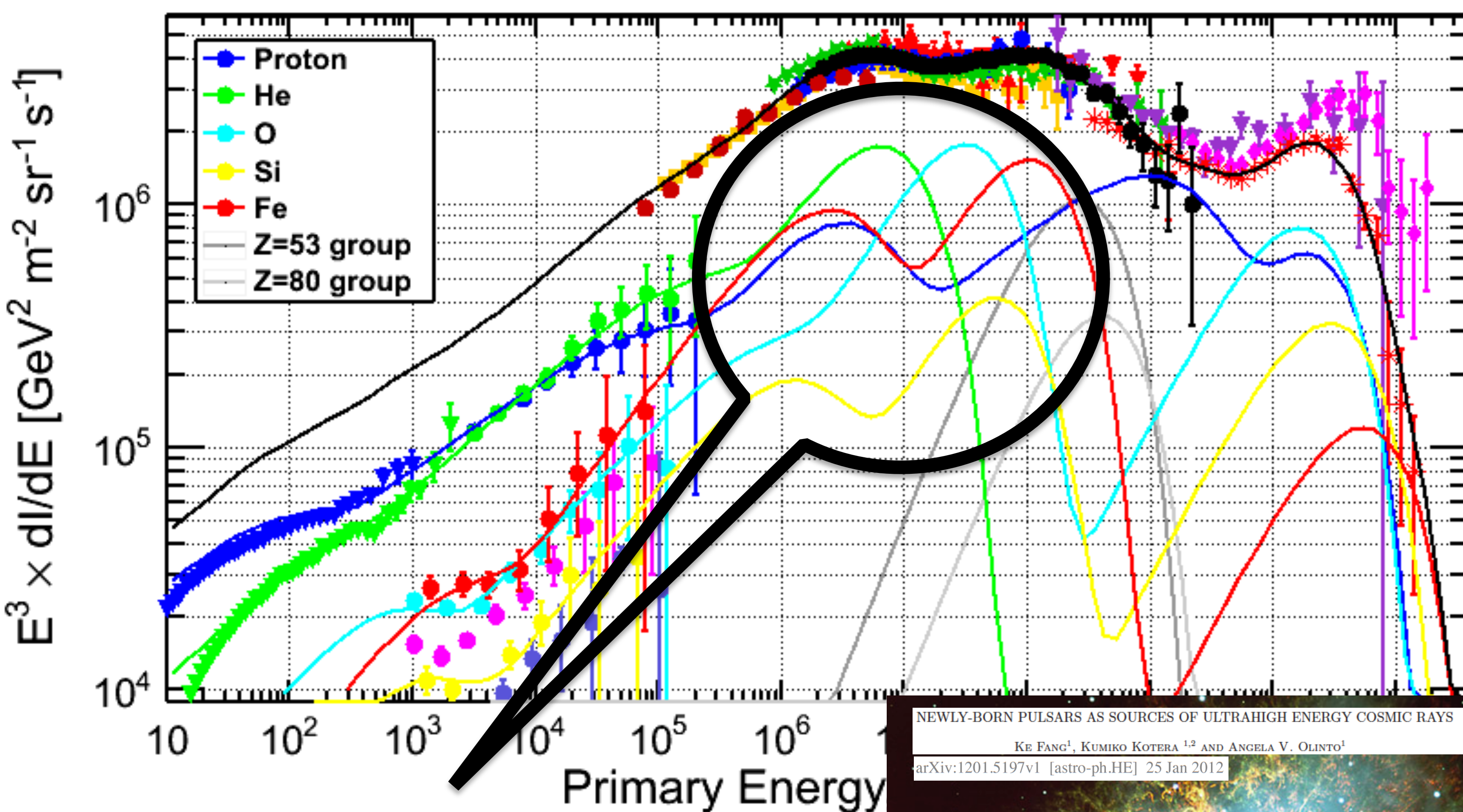

Fast spinning more massive stars

beamed structure

➔ Pulsar Wind Nebula systems

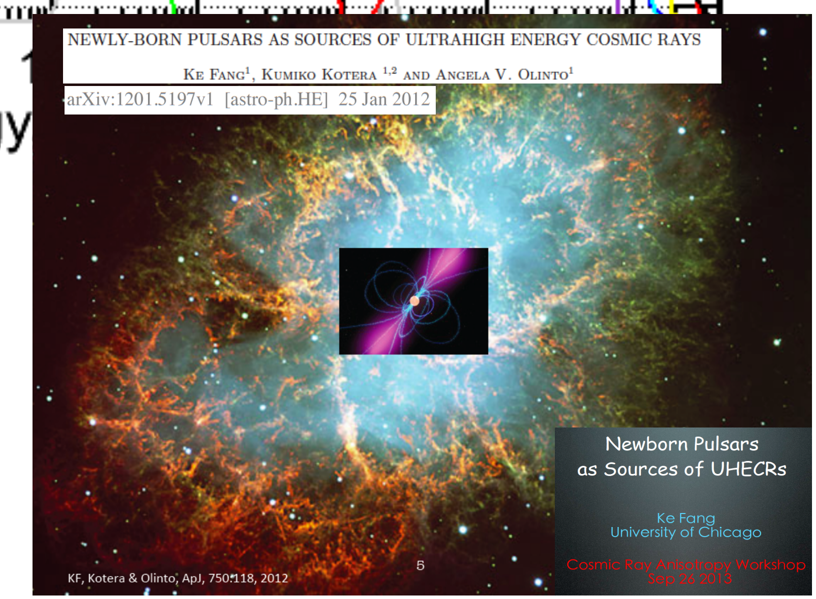

Observation of High-Energy Astrophysical Neutrinos in Three Years of IceCube Data

arXiv:1405.5303v2 [astro-ph.HE] 2 Jul 2014

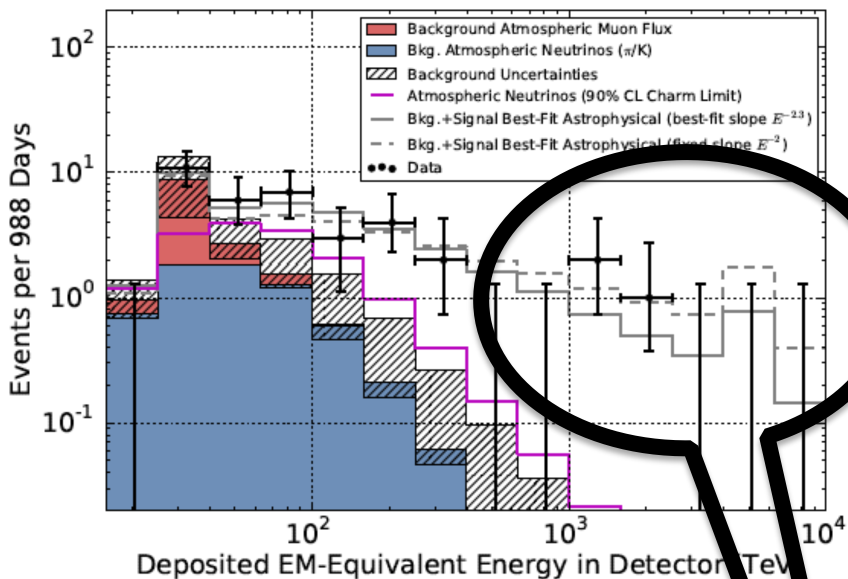

FIG. 2. Deposited energies of observed events with predictions. The hashed region shows uncertainties on the sum of all backgrounds. Muons (red) are computed from simulation to overcome statistical limitations in our background measurement and scaled to match the total measured background rate. Atmospheric neutrinos and uncertainties thereon are derived from previous measurements of both the π/K and charm components of the atmospheric ν_μ spectrum [9]. A gap larger than the one between 400 and 1000 TeV appears in 43% of realizations of the best-fit continuous spectrum.

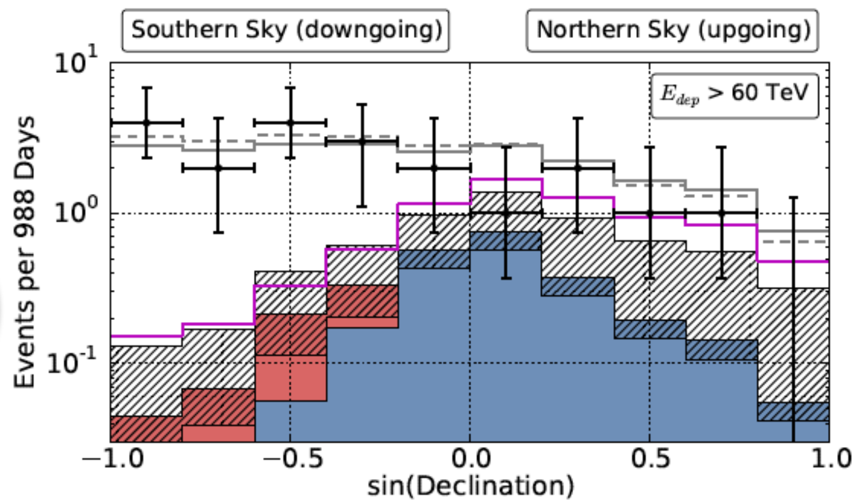

FIG. 3. Arrival angles of events with $E_{dep} > 60$ TeV, as used in our fit and above the majority of the cosmic ray muon background. The increasing opacity of the Earth to high energy neutrinos is visible at the right of the plot. Vetoing atmospheric neutrinos by muons from their parent air showers depresses the atmospheric neutrino background on the left. The data are described well by the expected backgrounds and a hard astrophysical isotropic neutrino flux (gray lines). Colors as in Fig. 2. Variations of this figure with other energy thresholds are in the online supplement [29].

1-2 PeV neutrinos as secondaries will come from ~ 20-40 PeV region of CR spectrum

6 source populations explain the observed CR spectrum and <lnA>

Source 1: The Sun (cutting off around 10 GeV)

Population 2: Old SNR (~10-20 kyrs old, e.g. IC443, W44, W28), cuts off ~100GeV

Population 3: The classical supernova cutting off around 100 TeV, ~1-3 in 100 yrs
Massive stars, circumstellar ejecta

Population 4: "Galactic PeVatron": PWN/Hypernovae, 1 in 1000 yrs ➔ TeV –PeV neutrinos
Fast spinning massive stars with mass 20-50 M_{sun}, beamed structure
found in star forming regions, live wild, die young,
leave a fast spinning pulsar behind

Population 5: "Galactic EeVatron": Hypernovae/GRB, 1 in 10000 yrs ➔ PeV neutrinos

Population 6: extragalactic Proton: superposed on population 5 ➔ PeV neutrinos

IceCube's TeV-PeV neutrinos are a mixture of Pop4 + Pop5 + Pop6 (galactic + extragalactic)